

## A trilinear stress-strain model for confined concrete

Alper Ilki†

*Istanbul Technical University, Civil Engineering Faculty, Structural and Earthquake Engineering Laboratory,  
34469, Maslak, Istanbul, Turkey*

Nahit Kumbasar‡

*Istanbul Technical University, Civil Engineering Faculty, Reinforced Concrete Division,  
34469, Maslak, Istanbul, Turkey*

Pinar Ozdemir†

*Istanbul Technical University, Civil Engineering Faculty, Mechanics Department,  
34469, Maslak, Istanbul, Turkey*

Toshibumi Fukuta‡†

*Building Research Institute, Tsukuba, Japan*

*(Received June 11, 2003, Accepted June 26, 2004)*

**Abstract.** For reaching large inelastic deformations without a substantial loss in strength, the potential plastic hinge regions of the reinforced concrete structural members should be confined by adequate transverse reinforcement. Therefore, simple and realistic representation of confined concrete behaviour is needed for inelastic analysis of reinforced concrete structures. In this study, a trilinear stress-strain model is proposed for the axial behaviour of confined concrete. The model is based on experimental work that was carried out on nearly full size specimens. During the interpretation of experimental data, the buckling and strain hardening of the longitudinal reinforcement are also taken into account. The proposed model is used for predicting the stress-strain relationships of confined concrete specimens tested by other researchers. Although the proposed model is simpler than most of the available models, the comparisons between the predicted results and experimental data indicate that it can represent the stress-strain relationship of confined concrete quite realistically.

**Key words:** buckling; columns (supports); confined concrete; ductility; reinforcement; strength; stress-strain curves.

---

† Assistant Professor  
‡ Professor  
‡† Doctor

## 1. Introduction

Against severe earthquakes, structures can survive by dissipating energy through inelastic deformations. Therefore, inelastic deformations are permitted during the design of reinforced concrete structures. To dissipate a considerable amount of energy, the structural members should exhibit ductile behaviour. This can be achieved by proper confinement of concrete sections by transverse reinforcement. Various experimental studies have confirmed that confinement provided by transverse reinforcement may significantly enhance the ductility and strength characteristics of concrete members (Kent and Park 1971, Sargin *et al.* 1971, Vallenias *et al.* 1977, Priestley *et al.* 1981, Park *et al.* 1982, Sheikh and Uzumeri 1982, Mugurama *et al.* 1983, Dilger *et al.* 1984, Ahmad and Shah 1982, 1985, Mander *et al.* 1988a, 1988b, Mugurama *et al.* 1990, Saatcioglu and Razvi 1992, Hsu and Hsu 1994, Cusson and Paultre 1995, Saatcioglu *et al.* 1995, Hoshikuma *et al.* 1997, Ilki *et al.* 1997, Braga and Laterza 1998, Assa and Nishiyama 1998). Several other researchers have carried out comparative compilation studies on the available stress-strain models proposed for confined concrete (Sheikh 1982, Sakai and Sheikh 1989, Chang and Mander 1994, Ilki 1999). Although many experimental and analytical studies have been carried out, experimental data, investigating the different ranges of the parameters that are effective on the behaviour, is still needed for a better understanding of the behaviour of confined concrete, particularly the post-peak branch of the stress-strain relationship. The available models include varying amounts of complexities and most of them are based on axial loading tests carried out on small size cylinders. In this study, the stress-strain behaviour of confined concrete is examined by testing nearly full size reinforced concrete columns with circular cross-sections. While evaluating the test results, the buckling and strain hardening of the longitudinal reinforcement are also taken into account. To determine the contribution of longitudinal reinforcing bars to the axial stresses after buckling, expressions given by Yalcin and Saatcioglu (2000) are taken into account. These expressions were derived by depending on the previous work done by Mau and El-Mabsout (1989) and Mau (1990). There are several parameters that effect the behaviour of confined concrete, such as the volumetric ratio, spacing, diameter and arrangement of confinement reinforcement, the shape and dimensions of the cross-section, the unconfined concrete compressive strength and loading rate. Consequently, it is almost impossible to model the stress-strain relationship of confined concrete realistically for all ranges of parameters that effect the behaviour. So, rather than trying to establish behavioural models that are valid for all cases, it may be more reasonable to use different models that are convenient for the case being dealt with. In this study, a simple stress-strain model, which is formed by three lines, is proposed to represent the axial behaviour of concrete confined by transverse reinforcement. The model is based on the experimental work carried out on nearly full size reinforced concrete members (Ilki *et al.* 1997, 1998). The proposed model predicts the stress-strain behaviour of confined concrete by determining the confined concrete strength and the strain corresponding to 85% of the confined concrete strength on the descending branch of the stress-strain curve. Unlike most of other available models proposed before, buckling of the longitudinal bars is also taken into account while predicting the descending branch of the stress-strain relationship. Besides being relatively simpler, comparisons with experimental data available in the literature indicate that the proposed model can predict the behaviour of confined concrete accurately. During comparisons, special emphasis is given to compressive strength, deformability, and the toughness characteristics. The validity of the model is limited to or around the range of parameters that were taken into account during the experimental study, which formed the basis for the proposed model. It should be

noted that the considered ranges of the variables in the experimental program cover most of the common cases in practice.

## 2. Inelastic compressive behaviour of longitudinal bars after buckling

For determination of the seismic performance of the reinforced concrete members, moment-curvature analysis is essential. In this type of analysis, it is important to know the stress-strain behaviour of reinforcing steel that includes the effect of buckling as well as the stress-strain behaviour of the concrete confined by transverse reinforcement. Although extensive work on the subject of confinement by transverse reinforcement has resulted in numerous empirical formulas on the spacing and diameter of transverse reinforcement, relatively few works have been reported regarding the buckling of the longitudinal reinforcing bars (Mau and El-Mabsout 1989). Test results on inelastic buckling of reinforcing bars show that buckling occurs near yielding load or during strain hardening (Mander 1983, Mau and El-Mabsout 1989, Monti and Nuti 1992, Rodriguez *et al.* 1999). During evaluation of experimental data on the axial behaviour of confined concrete columns, the axial behaviour of longitudinal reinforcing bars after buckling should also be taken into account. When this is not done, test data on confined concrete axial stress-axial strain relationship may include errors due to mistaken consideration of contribution of longitudinal reinforcement. Consequently, any proposed empirical equation based on this type of data may inherently include errors. In this study, for determining the contribution of longitudinal bars to the axial stresses after buckling, the expressions given by Yalcin and Saatcioglu (2000), which were derived mainly from the work done by Mau and El-Mabsout (1989) and Mau (1990), are taken into account. A schematic representation of stress-strain relationships for reinforcing steel in compression is given in Fig. 1. In this figure,  $f_y$  is the yield stress and  $s/\phi_l$  is the ratio of unsupported bar length between two ties to its diameter. As seen in Fig. 1, stress-strain behaviour of reinforcing steel in compression can be modeled considering three different ranges of  $s/\phi_l$  ratio.

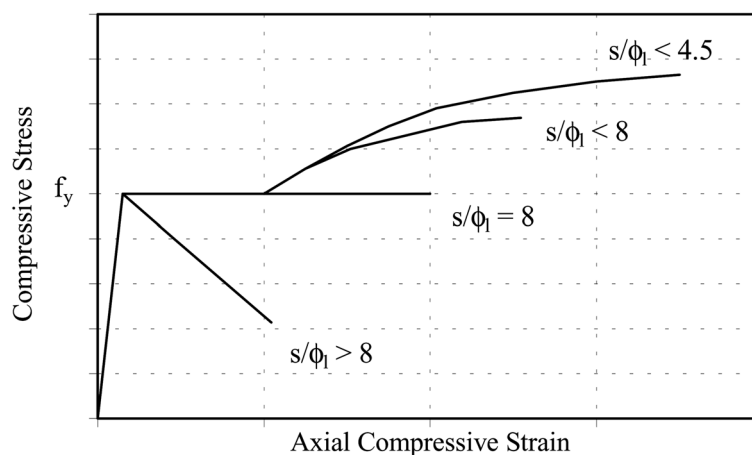


Fig. 1 Stress-strain relationship for reinforcing steel in compression considering buckling (Yalcin and Saatcioglu 2000)

### 2.1 Range 1 : $s/\phi_l \leq 4.5$

If  $s/\phi_l$  is smaller than 4.5, then the stress-strain relationship in compression can be assumed to be identical to that in tension with complete strain hardening.

### 2.2 Range 2 : $4.5 < s/\phi_l < 8$

In this range, the stress-strain relationship exhibits strain hardening. However, the strain hardening curve is lower than the tension curve. The difference between compression and tension curves increases as  $s/\phi_l$  ratio approaches 8. The compressive steel stress after reaching strain hardening can be determined by Eq. (1), where the limiting values for stress,  $f_{s/Du}$ , and strain,  $\varepsilon_{s/Du}$ , are given by Eqs. (2) and (3). In these equations  $f_{sh}$  and  $\varepsilon_{sh}$  are the axial stress and the corresponding strain of steel reinforcement at the beginning of strain hardening,  $f_{su}$  and  $\varepsilon_{su}$  are the ultimate strength and the corresponding strain, and  $\sigma_s$  and  $\varepsilon_s$  are the compressive stress and corresponding strain of the steel reinforcement at any step of the loading.

$$\sigma_s = f_y + (f_{s/Du} - f_{sh}) \left[ \frac{2(\varepsilon_s - \varepsilon_{sh})}{\varepsilon_{s/Du} - \varepsilon_{sh}} - \left( \frac{\varepsilon_s - \varepsilon_{sh}}{\varepsilon_{s/Du} - \varepsilon_{sh}} \right)^2 \right] \quad (1)$$

$$f_{s/Du} = f_{sh} + (f_{su} - f_{sh}) [48e^{-0.9(s/\phi_l)}] \quad (2)$$

$$\varepsilon_{s/Du} = \varepsilon_{sh} + (\varepsilon_{su} - \varepsilon_{sh}) [6e^{-0.4(s/\phi_l)}] \quad (3)$$

### 2.3 Range 3 : $s/\phi_l \geq 8$

In this range, the reinforcing steel becomes unstable as soon as the yield point is reached. Compressive stress can be assumed to decrease linearly as the strain increases. The slope of the descending branch can be determined based on the  $s/\phi_l$  ratio by using Eq. (4). In this equation,  $\varepsilon_y$  is the yield strain for reinforcing steel. Limiting values for stress,  $f_{s/Du}$ , and strain,  $\varepsilon_{s/Du}$ , are given by Eqs. (5) and (6).

$$\sigma_s = f_y - (\varepsilon_s - \varepsilon_y) \left[ -23000 + 11000 \ln \left( \frac{s}{\phi_l} \right) \right] \quad (4)$$

$$f_{s/Du} = 28 \left( \frac{s}{\phi_l} \right)^{-1.7} f_y \quad (5)$$

$$\varepsilon_{s/Du} = \left[ 40 - 6 \ln \left( \frac{s}{\phi_l} \right) \right] \varepsilon_y \quad (6)$$

Considering the observations during the experimental work outlined in this paper, as well as other available experimental data in the literature, these ranges are quite reasonable. Note that, the stress quantities used in the above expressions are in MPa and further details of the stress-strain model for reinforcing steel can be found elsewhere (Yalcin and Saatcioglu 2000).

### 3. Outline of the experimental work and interpretation of the experimental data

The proposed stress-strain relationship for confined concrete is based on the experimental work carried out by Ilki *et al.* (1997, 1998) in the Structure Laboratory of the Building Research Institute in Tsukuba, Japan. In this experimental study, nearly full size reinforced concrete members with the approximate concrete compressive strength of 20 MPa were tested under concentric compression. The cross-section of the specimens was circular, with diameters of 250 and 200 mm. The height of the specimens was 1000 mm. The test variables were the spacing, diameter, and type of the confinement reinforcement, whose volumetric ratio varied between 0.7 and 2%. In this experimental study, the diameter of the confinement reinforcement, either hoops or spirals, varied between 6 and 13 mm and the spacing varied between 26 and 161 mm, while all specimens had 6 deformed bars of 16 mm diameter as longitudinal reinforcement. Consequently the geometric ratios of longitudinal reinforcement were 0.025 and 0.038 for the specimens with the diameter of 250 mm and for one specimen with the diameter of 200 mm, respectively. The specimens were given designations according to the diameter of the specimen and the diameter, spacing and type (hoop or spiral) of the confinement reinforcement. For example, D250H10@71 is the designation of a specimen with **250 mm** diameter that had **Hoops** with a diameter of **10 mm** and spacing of **71 mm** as confinement reinforcement in the testing zone. The general appearance and characteristics of the specimens are shown in Fig. 2 and Table 1, respectively. The core diameters measured from the outer sides of the lateral reinforcement,  $D_c$ , were 215 and 200 mm for the specimens with 250 and 200 mm diameter, respectively. The middle one-third heights of the specimens were designed as the testing zone. Outside the testing zone, the volumetric ratio of confinement reinforcement was doubled, so that the specimens were forced to fail in the testing zone, where all the instrumentation was installed. In order to prevent direct loading of longitudinal bars, there was a concrete cover of 30 mm at the bottom and top surfaces of the specimens.

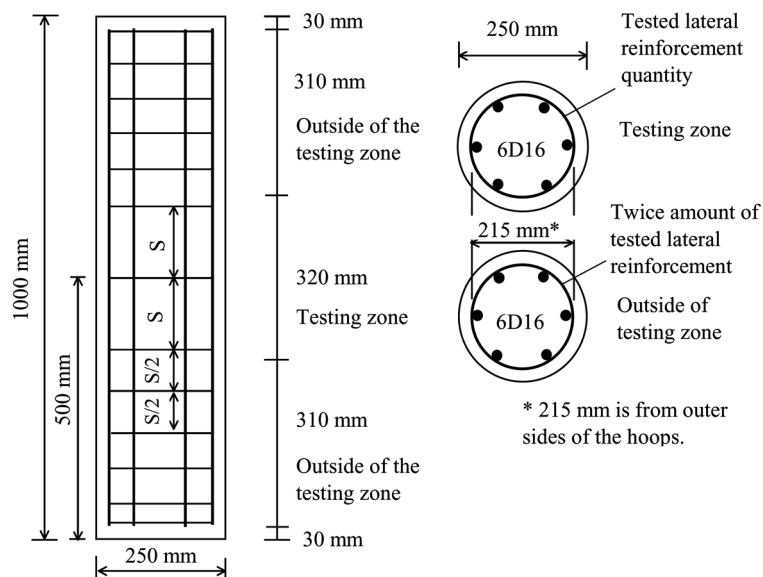


Fig. 2 General appearance of the specimens

Table 1 Properties of the specimens tested by Ilki *et al.* (1997)

Specimen No	Specimen	Transverse reinforcement in test zone	Volumetric ratio $\rho_{sh}$	Yield strength of transverse bars $f_{yh}$ MPa	$\rho_{sh} \times f_{yh}$ MPa	Transverse reinforcement out of test zone
1	D250H6@50	D6@50	0.0105	447	4.69	D6@25
2	D250H10@143	D10@143	0.0102	320	3.26	D10@70
3	D250H6@34	D6@34	0.0155	447	6.93	D6@17
4	D250H10@95	D10@95	0.0154	320	4.93	D10@45
5	D250H13@161	D13@161	0.0153	325	4.97	D13@80
6	D250H6@26	D6@26	0.0202	447	9.03	D10@30
7	D250H10@71	D10@71	0.0206	320	6.59	D10@35
8	D250H13@121	D13@121	0.0204	325	6.63	D13@60
9	D250S10@95	D10@95	0.0154	320	4.93	D10@45
10	Unconfined	No	0	No	0	No
11	D250H6@75	D6@75	0.0070	447	3.13	D6@35
12	D200H10@95	D10@95	0.0165	320	5.28	D10@45

Table 2 Concrete mix-proportion

Cement kg/m <sup>3</sup>	Water kg/m <sup>3</sup>	Fine aggregate kg/m <sup>3</sup>	Coarse aggregate kg/m <sup>3</sup>	Air-entraining admixture kg/m <sup>3</sup>
282	189	868	874	3.02

Table 3 Mechanical characteristics of steel reinforcement

Diameter mm	Yield strength, $f_y$ MPa	Tensile strength, $f_{su}$ MPa	$f_{su}/f_y$	Ultimate deformation, $\epsilon_{su}$
16	347	500	1.44	0.28
13	325	463	1.42	0.31
10	320	428	1.34	0.29
6	447	654	1.46	Not available

Ready mixed concrete with a maximum aggregate size of 10 mm was used for all specimens. The concrete mix-proportion is given in Table 2. The average standard cylinder compressive strength,  $f'_c$ , at the age of 28 days was 19.2 MPa and the average strain corresponding to peak stress was 0.0022. In this study, the member concrete compressive strength,  $f'_{co}$ , is assumed as  $0.75 f'_c$ . 16 mm diameter deformed bars were used as longitudinal reinforcement for all specimens, while 6, 10 and 13 mm diameter deformed bars were used for transverse reinforcement. The average yield and tensile stresses, and ultimate strains of steel reinforcement are given in Table 3.

Concentric compression was applied by a loading machine with the capacity of 10000 kN. In order to prevent premature failure at the top and bottom ends of the specimens, steel tube collars with an inside diameter of 276 mm and a height of 150 mm, were placed around the end zones of

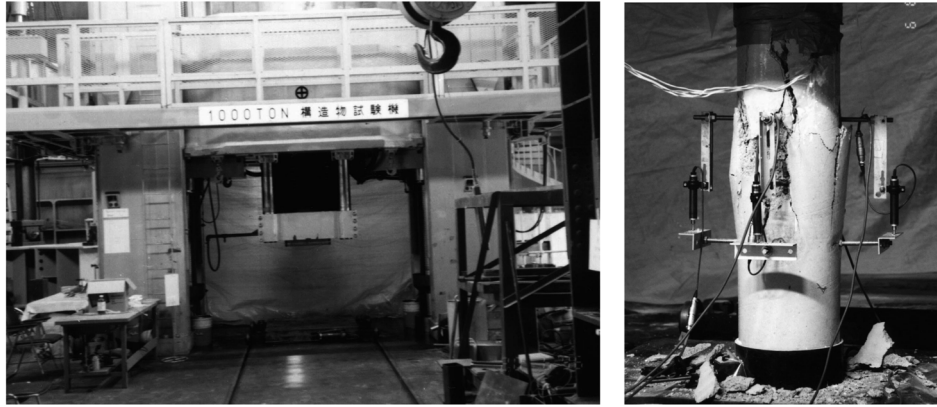


Fig. 3 Loading machine and an appearance during testing

the specimens. For measuring average vertical strains in the testing zone, four displacement transducers, with the displacement capacity of 25 mm, were mounted vertically around the perimeter of the testing zone of the specimens with 90 degree angle intervals. The appearances of the loading machine and a specimen during testing are shown in Fig. 3. The analysis of the measurements of these transducers assured that the loading was exactly concentric until large levels of axial strains. The gauge lengths for these displacement transducers were 320 mm. Strain gauges were also bonded on the longitudinal and transverse bars, so that the longitudinal and transverse steel stresses and strains could be determined. Measurements of load, displacements and strains were recorded by using a data logger, and the data was analysed by using computers. During the evaluation of the test results, average values that were obtained by the displacement transducers or strain gages were considered.

While determining the contribution of longitudinal bars to the axial loads resisted, both strain hardening and inelastic buckling of the reinforcement were taken into account, Fig. 1. While interpreting the experimental data, the contribution of longitudinal reinforcement was taken into account by Eq. (7).

$$F_s = A_s \sigma_s \quad (7)$$

In Eq. (7),  $F_s$  is the compression force resisted by the longitudinal reinforcement,  $\sigma_s$  is the compressive stress and  $A_s$  is the total cross-sectional area of the longitudinal reinforcement. For each step of loading,  $\sigma_s$  was determined by considering Fig. 1 and the expressions given by Yalcin and Saatcioglu (2000).

For all of the specimens, it was observed that the cover concrete spalled off around the axial strain level, at which longitudinal reinforcing bars yielded due to compression. Consequently, while utilizing the test results, the gross concrete cross-section was taken into account until the longitudinal reinforcing bars yielded, and after that only the core concrete was considered to resist compression.

#### 4. Summary of the test results

Although, it is not aimed to present all experimental data in this paper, for demonstrating main behavioural characteristics of confined concrete columns, which formed the basis of the proposed stress-strain model, several experimental results are highlighted with emphasis on the failure patterns of the specimens. Mainly three different types of failure patterns were observed during tests. When the spacing of transverse reinforcement was very small ( $s < 4\phi_l$ ), the transverse bars fractured at relatively high axial strains and no buckling was observed for longitudinal reinforcing bars, Fig. 4(a). When the spacing was between 4 and  $7\phi_l$ , the longitudinal bars buckled at relatively larger axial strains, such that compressive strains exceeded the strain level, at which strain hardening began. When the spacing was higher ( $s > 7\phi_l$ ), the longitudinal bars buckled at relatively lower levels of axial strain at around yield point, Fig. 4(b). Between these three different failure types, the behaviour of confined concrete is almost identical for the first and second types of failures until high level of axial strains (0.04~0.05). However, for the third type of failure, the slope of the descending branch of the stress-strain relationship of confined concrete is much steeper. Consequently, since the behaviour after the axial strain level of 0.04~0.05 is not practically meaningful, the behaviour can be examined for two different cases; when the longitudinal bars do not lose their stability prematurely ( $s \leq 7\phi_l$ ) or when they are buckled at around yield point, ( $s > 7\phi_l$ ). So, according to the experimental data obtained in this study, the spacing, which seems as a kind of transition border between these two cases, is assumed as  $7\phi_l$ .

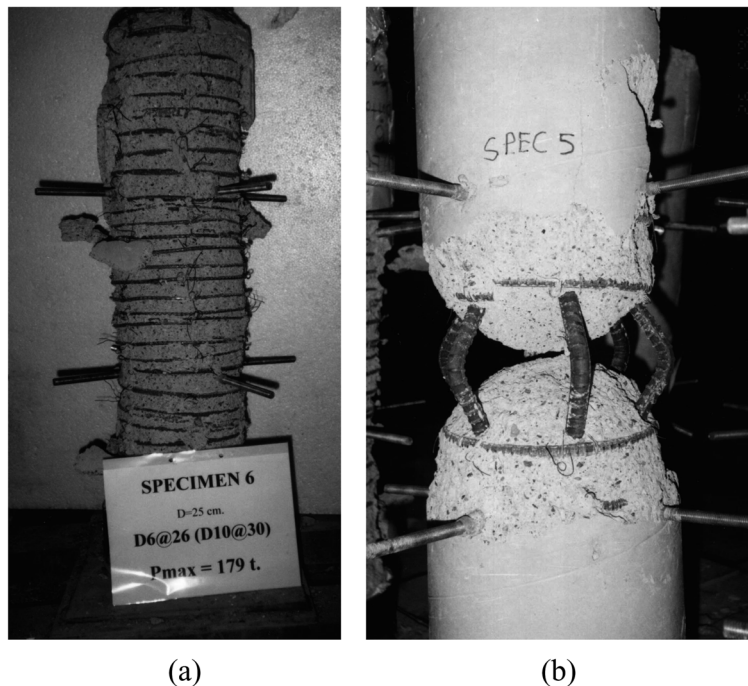


Fig. 4 Typical failure patterns

For demonstrating the effect of volumetric ratio of transverse reinforcement on the behaviour, the dimensionless experimental stress-strain relationships are presented in Fig. 5. In this figure,  $\sigma_c$  is the concrete compressive stress,  $f'_{co}$  and  $f'_{cc}$  are the unconfined and confined concrete compressive strengths of the member and  $\rho_{sh}$  is the volumetric ratio of the transverse reinforcement. As seen in this figure, while buckling of the longitudinal reinforcement was observed around or after the axial strain level of 0.04 for the specimens with transverse reinforcement spacing less than  $6\phi_t$ , when

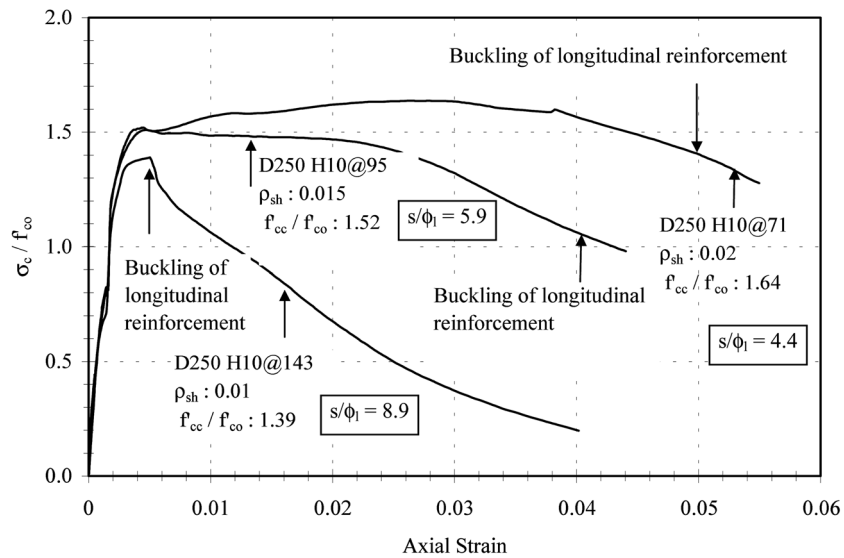


Fig. 5 The effects of volumetric ratio of transverse bars on the behaviour

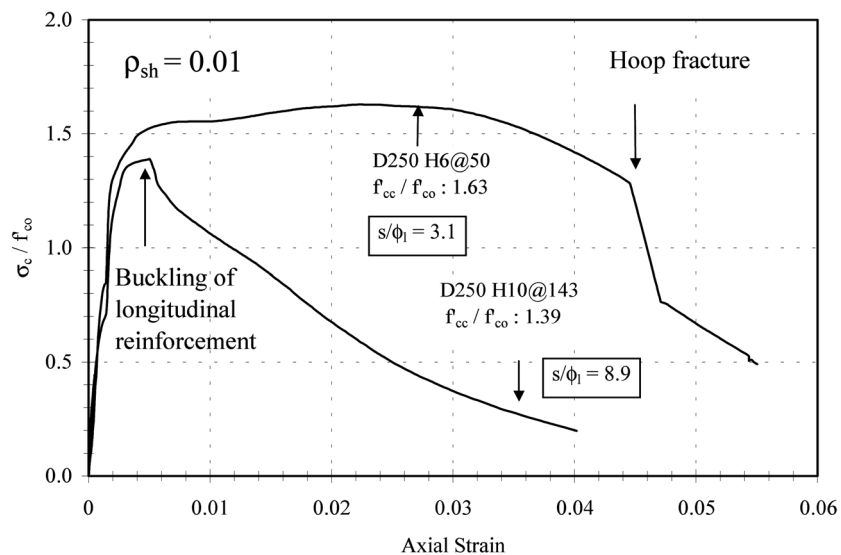


Fig. 6 The effects of spacing of transverse bars on the behaviour

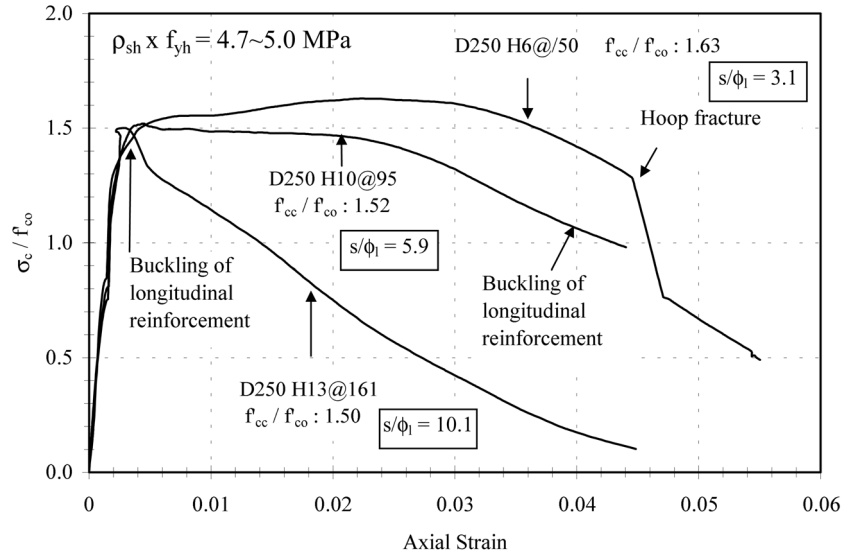


Fig. 7 The effects of spacing of transverse bars on the behaviour for specimens having the  $\rho_{sh} \times f_{yh}$  value of 4.7~5.0

spacing was higher ( $\sim 9\phi_l$ ), early loss in strength was observed due to buckling of the longitudinal bars in the early stages of inelastic range. Note that, the slope of the descending branch is much steeper in this case. Besides these, it can be seen that the compressive strength was also increased significantly as a function of the confinement. The effect of the spacing of the transverse bars for the specimens with the same volumetric ratio is presented in Fig. 6. As seen in this figure, although specimens had equal volumetric ratios of transverse reinforcement, their performances were totally different. Both the compressive strength and the ductility were improved much more for the specimen with smaller hoop spacing. The failure patterns were also different, which naturally affected the slope of descending branch significantly. For eliminating the effect of different yield strengths of transverse bars with different diameters, a more realistic comparison is given in Fig. 7 for the specimens that approximately had the same value of  $\rho_{sh} \times f_{yh}$ , where  $f_{yh}$  is the yield strength of transverse bars. As seen in this figure, when the specimens having approximately equal values of  $\rho_{sh} \times f_{yh}$  are compared, both the compressive strength and ductility characteristics are better when the spacing of transverse bars is relatively smaller. However, it should be noted that, the enhancement in compressive strength is not as much pronounced as the enhancement in ductility.

In Figs. 5, 6 and 7, the axial strains, at which buckling of longitudinal reinforcement and/or fracture of transverse reinforcement were observed, are marked.

## 5. Trilinear stress-strain relationship

A simple trilinear stress-strain relationship is proposed for the axial behaviour of normal strength concrete confined by transverse reinforcement based on experimental results. The most important characteristics of confined concrete are enhancement in compressive strength and ductility. Enhanced ductility characteristics can also be defined as the reduced slope of the descending branch

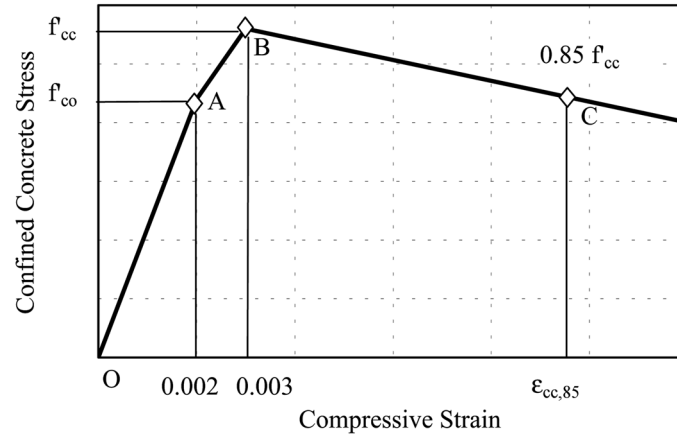


Fig. 8 Proposed stress-strain relationship

of the stress-strain relationship and, consequently, a higher ultimate axial strain. The proposed stress-strain relationship is composed of three lines as shown in Fig. 8. The initial line connects the origin to point A that represents the strength of unconfined concrete and corresponding strain,  $\epsilon_{co} = 0.002$ . The second line connects point A to point B that represents the confined concrete strength and the corresponding strain, which is assumed to be  $0.003$ . The third line is between point B and point C, which corresponds to the 15% drop of the confined concrete strength on the descending branch. The slope of the third line is determined according to the expected failure pattern, which may be either fracture of the transverse bars or buckling of the longitudinal bars.

It is known that confined concrete characteristics are particularly important when inelastic behaviour of reinforced concrete members is under investigation. Consequently, the predicted behaviour of confined concrete in the elastic range should not necessarily be as accurate as the behaviour in the inelastic range. So, for the sake of simplicity and considering that the effect of more accurate representation of this portion of the stress-strain relationship has negligible effects on the overall behaviour, as seen in Fig. 8, a simple line is used for this portion of the stress-strain relationship, which represents the behaviour until unconfined concrete strength, point A in Fig. 8. As can also be understood from Fig. 8, in this portion of the stress-strain model, the confined concrete stresses can be determined by Eq. (8).

$$\sigma_c = \frac{f'_{co}}{0.002} \epsilon_c \quad (8)$$

In Eq. (8),  $\sigma_c$  and  $\epsilon_c$  are the axial concrete stress and the corresponding axial strain at any stage of loading, and  $f'_{co}$  is the unconfined concrete compressive strength of the member. Most of the available models propose empirical expressions for the strain corresponding to confined concrete strength, however, when the curves in Figs. 5, 6 and 7 are taken into account, it can be seen that around the confined concrete strength the axial strains vary too much. Consequently, it is really difficult to decide which value of the axial strain should be considered as the strain corresponding to confined concrete strength. This difficulty is also reflected by the much-scattered values of strains corresponding to the confined concrete strength predicted by the models proposed by various researchers for the identical confined concrete members (Ilki and Kumbasar 2001). Therefore, in

this study, rather than proposing an expression for the strain corresponding to confined concrete strength,  $\varepsilon_{cc}$ , an expression is proposed for the strain corresponding to the stress that is 85% of the confined concrete strength,  $\varepsilon_{cc,85}$ , on the descending branch of the stress-strain relationship. In this model, the strain corresponding to confined concrete compressive strength is assumed to be 0.003 for all cases. So, between point A (0.002,  $f'_{co}$ ) and point B (0.003,  $f'_{cc}$ ), the confined concrete stresses can be calculated by Eq. (9).

$$\sigma_c = 1000(f'_{cc} - f'_{co})\varepsilon_c + 2(1.5f'_{co} - f'_{cc}) \quad (9)$$

The test data showed that the confined concrete compressive strength,  $f'_{cc}$ , can be determined as a function of the effective lateral pressure provided by confinement,  $f'_l$ , and the member unconfined concrete compressive strength,  $f'_{co}$ . Statistical evaluation of the test data obtained by Ilki *et al.* (1997) led to Eq. (10) for the confined concrete strength, which is independent of the failure type.

$$f'_{cc} = f'_{co} \left[ 1 + 4.54 \frac{f'_l}{f'_{co}} \right] \quad (10)$$

Based on the experimental data and observations, a spacing of  $7\phi_l$  between transverse bars is assumed as a threshold value that can be used for predicting the failure pattern; namely for predicting whether the longitudinal reinforcement will be prematurely buckled or not, in the practically achievable ranges of axial strains. For these two main failure patterns, statistical analysis of the experimental data obtained by Ilki *et al.* (1997) resulted in Eqs. (11) and (12), for the cases whether premature longitudinal reinforcement buckling is present or not, respectively. For the cases, when spacing of the transverse bars is too high, to obtain a  $\varepsilon_{cc,85}$  value close to unconfined concrete, the minimum value of  $\varepsilon_{cc,85}$  in Eq. (11) should be 0.0035.

$$s > 7\phi_l \quad \varepsilon_{cc,85} = \varepsilon_{co} \left[ 1 + 110 \frac{f'_l}{f'_{co}} \right] \left[ \frac{7\phi_l}{s} \right]^2 \geq 0.0035 \quad (11)$$

$$s \leq 7\phi_l \quad \varepsilon_{cc,85} = \varepsilon_{co} \left[ 1 + 110 \frac{f'_l}{f'_{co}} \right] \quad (12)$$

In these equations, the effective lateral pressure provided by confinement,  $f'_l$ , can be calculated by Eq. (13), where  $f_l$  is the lateral pressure and  $k_e$  is the confinement effectiveness coefficient.

$$f'_l = k_e f_l \quad (13)$$

$k_e$  can be determined as the ratio of effectively confined cross-sectional area,  $A_e$ , to confined cross-sectional area calculated from center to center of transverse bars,  $A_{cc}$ , and can be determined by Eq. (14).

$$k_e = \frac{A_e}{A_{cc}} \quad (14)$$

In this study, like Mander *et al.* (1988b) and Sheikh and Uzumeri (1982), the effectively confined

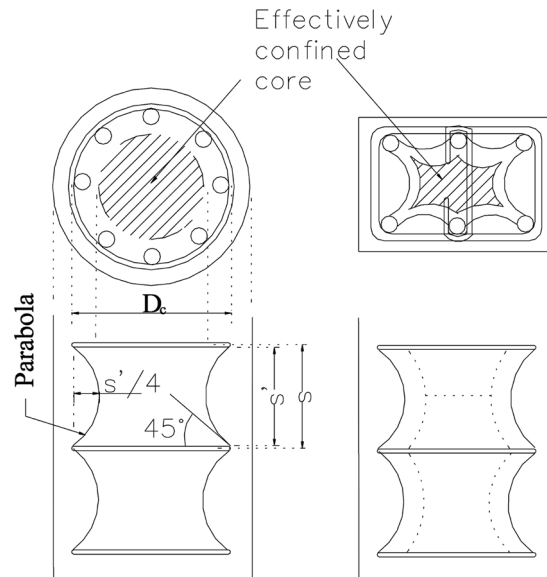


Fig. 9 Determination of effectively confined core,  $A_e$

core area,  $A_e$ , is determined as shown in Fig. 9. For circular cross-sections,  $A_e$  and  $f_l$  can be obtained by Eqs. (15) and (16), respectively. In Eqs. (15) and (16),  $s$  and  $s'$  are the axial and clear spacing between transverse reinforcing bars,  $D_c$  is the diameter of the confined cross-section and  $A_{sh}$  is the cross-sectional area of the transverse reinforcing bars. For square and rectangular cross-sections,  $A_e$  and  $f_l$  can be determined as given by Mander *et al.* (1988a).

$$A_e = \frac{\pi}{4} D_c^2 \left[ 1 - \frac{s'}{2D_c} \right]^2 \tag{15}$$

$$f_l = \frac{2A_{sh}f_{yh}}{D_c s} \tag{16}$$

Permitted ultimate axial strain of confined concrete may depend on the type of the analysis and acceptable level of damage for the analysed member or non-structural members around the analysed member. Consequently, no specific limit for ultimate axial strain is given in this paper. The decision on the ultimate axial strain should better be given according to the case being dealt by considering the level of strength loss on the descending branch of the stress-strain relationship as well as the other practical limitations for ultimate axial strain.

## 6. Comparisons with experimental results of this research

Although it may naturally be expected that the stress-strain relationships determined by the proposed model fit well with the experimental data that the expressions and rules of the proposed model are based on, the level of agreement between the stress-strain relationships predicted by

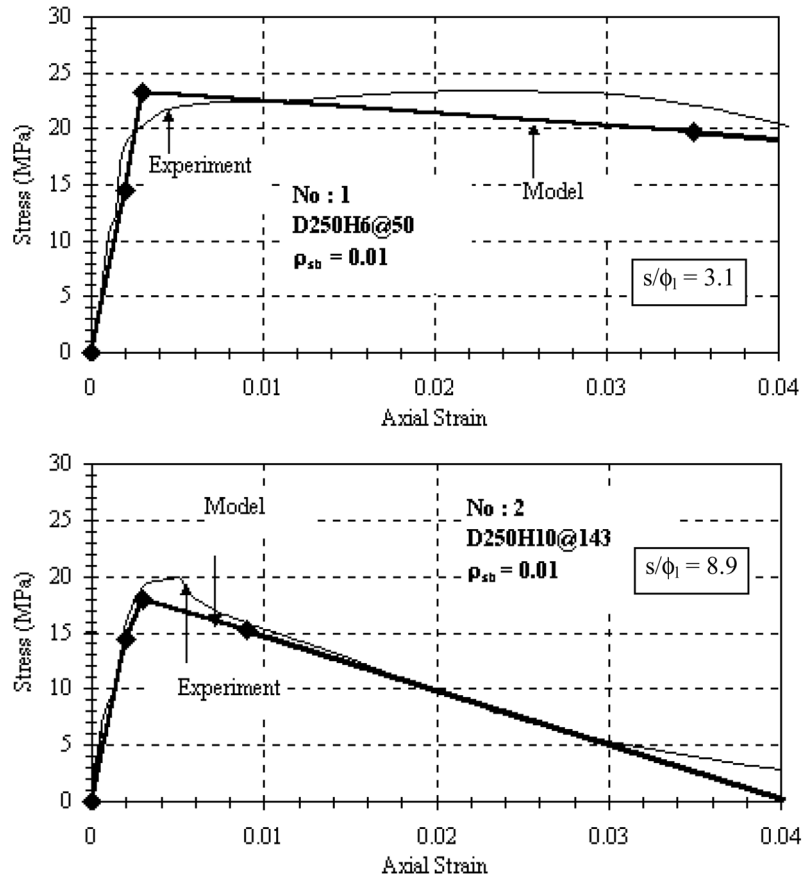


Fig. 10 Predicted and experimental stress-strain relationships for specimens with the transverse reinforcement volumetric ratio of 0.01

the proposed model and the experimental ones is a good indicator of the reliability of the model. Consequently, the stress-strain relationships predicted by the proposed model and those obtained experimentally by Ilki *et al.* (1997) are presented in Fig. 10 for Specimens D250H6@50 and D250H10@143, in Fig. 11 for Specimens D250H10@95 and D250H13@161, and in Fig. 12 for specimens D250H13@121 and D250H6@75. These comparisons show that both confined concrete compressive strength and ductility characteristics of the specimens are predicted satisfactorily by the proposed model. For providing a numerical comparison of overall predicted and observed behaviour, the areas under the predicted and experimental stress-strain curves at various levels of axial strain are presented in Fig. 13. With the exception of Specimen 8 (D250H13@121), the areas determined experimentally and by the proposed model are almost identical. The almost-perfect representation of the proposed model of the areas under the stress-strain curves can be seen during all phases of the loading curve until very large axial strains. Consequently, besides being simple and easy to use, the proposed model can represent the overall axial stress-axial strain behaviour of reinforced concrete members realistically, even when the spacing of transverse bars is not small enough to prevent buckling of the longitudinal reinforcement.

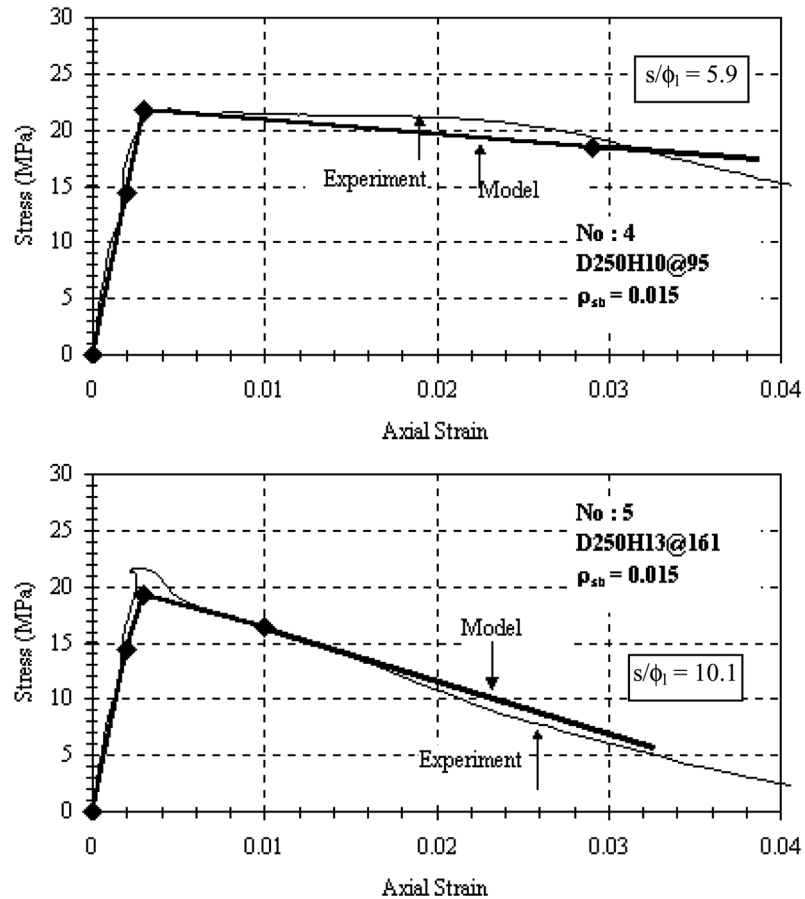


Fig. 11 Predicted and experimental stress-strain relationships for specimens with the transverse reinforcement volumetric ratio of 0.015

This leads to the conclusion that when the related characteristics of the examined members such as unconfined concrete strength, volumetric ratio and spacing of transverse reinforcement, cross-sectional shape and configuration of longitudinal reinforcement are in or around the range of the variables of the specimens tested by Ilki *et al.* (1997), the proposed model can be used for predicting the overall axial stress-axial strain behaviour. These ranges are 26-161 mm for the spacing of transverse reinforcement, 1.6-10.1 for the  $s/\phi_1$  ratios, 0.007-0.020 for the volumetric ratio of transverse reinforcement, 320-447 MPa for the yield strength of transverse bars. The standard cylinder strength for the concrete mix was 19.2 MPa.

## 7. Comparisons with experimental results available in the literature

There is a wide collection of experimental results on the behaviour of confined concrete available in the literature. The reliability of the proposed model is further investigated by comparisons with the experimental results obtained by Sheikh and Toklucu (1993), Mander *et al.* (1988a), Hoshikuma

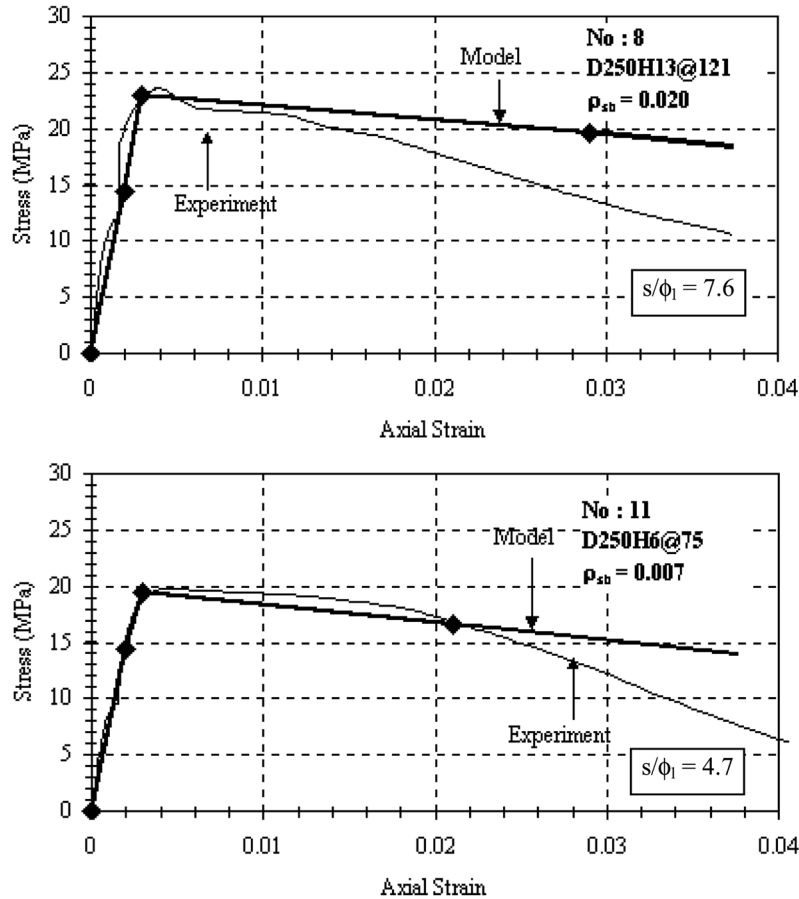


Fig. 12 Predicted and experimental stress-strain relationships for specimens with the transverse reinforcement volumetric ratio of 0.020 and 0.007

*et al.* (1997) and Ahmad and Shah (1982). While selecting the specimens to utilize for comparisons, cross-sectional shapes, unconfined concrete strength, sizes of the specimens, yield strength of transverse reinforcement and levels of lateral confinement pressure are considered as selection criteria. Specimens tested by Hoshikuma *et al.* (1997) were confined by hoops, those tested by Mander *et al.* (1988a) and Ahmad and Shah (1982) were confined by spirals, while both spirally and hoop confined specimens were tested by Sheikh and Toklucu (1993). Characteristics of the specimens considered for comparison are given in detail in Table 4. In this table,  $\phi_t$  is the diameter of transverse bars. For the specimens given in Table 4, confined concrete compressive strength and axial strain corresponding to 85% of confined concrete strength on the descending branch are predicted by using Eqs. (10), (11) and (12). The distribution of the experimental and predicted values of confined concrete strength and axial strain values corresponding to 85% of the confined concrete strength on the descending branch are illustrated in Fig. 14. For a more detailed comparison of the predicted and experimental values, the confined concrete strength values predicted by using Eq. (10),  $f'_{cc,model}$ , and axial strain values corresponding to 85% of the confined concrete strength on the descending branch predicted either by Eq. (11) or (12),  $\epsilon_{cc,85,model}$ , according

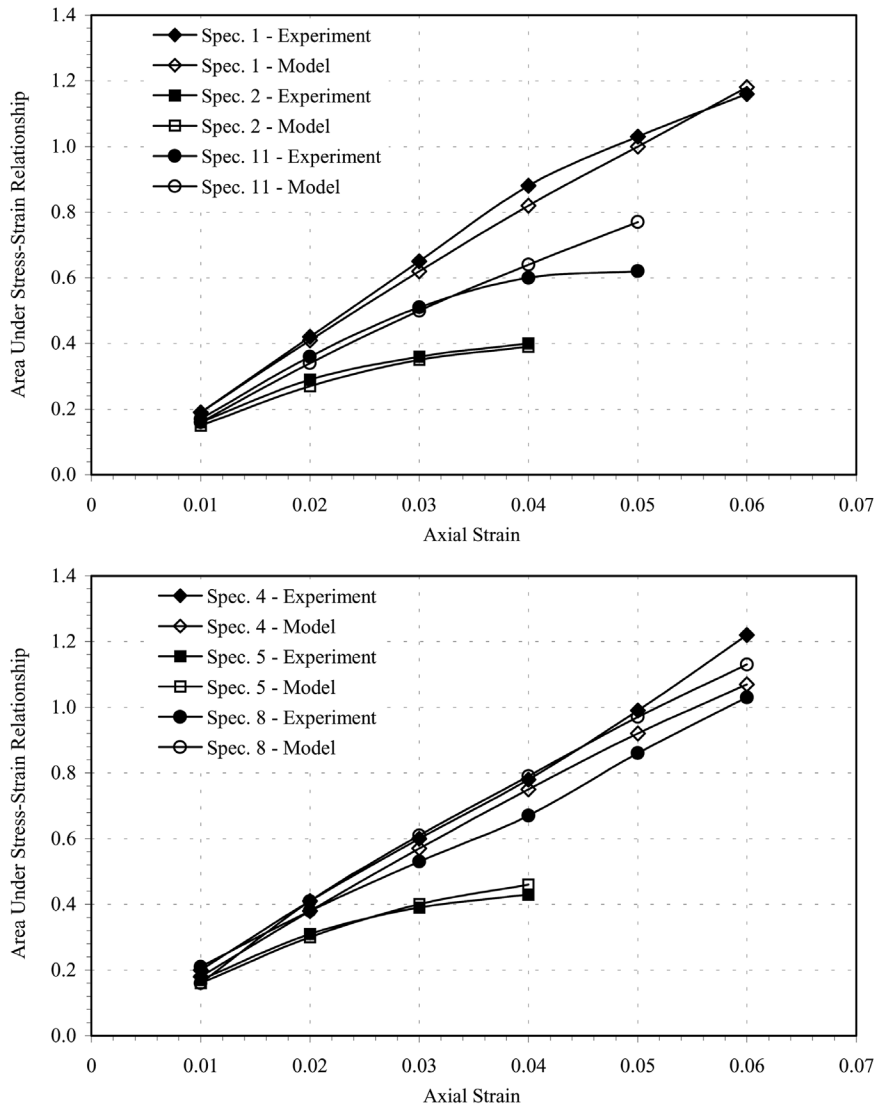


Fig. 13 Areas under the experimental and predicted stress-strain relationships

to the ratio of spacing of transverse reinforcement to the diameter of longitudinal bars, are given together with the corresponding experimental data in Table 5. As seen in this table, a good agreement is present between the predicted values and the experimental data, particularly for the confined concrete strength. The average of the ratio of the experimental to the predicted confined concrete strength values is 1.07 with a standard deviation of 0.15. The average of the ratio of experimental to predicted axial strain values corresponding to 85% of the confined concrete strength on the descending branch is also 1.07 with a standard deviation of 0.39.

Table 4 Characteristics of the specimens tested by other researchers

Resear- cher	Spec.	hoop	$f'_c$	$f'_{co}$	$\epsilon_{co}$	$\rho_{sh}$	$f_{yh}$	$D_c$	$\phi_t$	$s$	$s'$	$A_{cc}$	$A_e$	$k_e$	$f_i$	$f'_i$
		spiral	MPa	MPa			MPa	mm	mm	mm	mm	mm <sup>2</sup>	mm <sup>2</sup>		MPa	MPa
S-T	1	spiral	35.9	30.5	0.002	0.0230	452	302	10	56	46	71595	61105	0.853	4.196	3.581
S-T	2	spiral	35.9	30.5	0.002	0.0169	452	302	10	76	66	71595	56803	0.793	3.092	2.453
S-T	3	spiral	35.9	30.5	0.002	0.0115	452	302	10	112	102	71595	49456	0.691	2.098	1.449
S-T	4	spiral	35.9	30.5	0.002	0.0085	452	302	10	152	142	71595	41888	0.585	1.546	0.904
S-T	5	spiral	35.9	30.5	0.002	0.0115	607	304	8	56	48	72547	61544	0.848	3.583	3.039
S-T	6	spiral	35.9	30.5	0.002	0.0085	607	304	8	76	68	72547	57227	0.789	2.640	2.082
S-T	7	spiral	35.9	30.5	0.002	0.0058	607	304	8	112	104	72547	49851	0.687	1.791	1.231
S-T	8	spiral	35.9	30.5	0.002	0.0059	593	306	5.7	56	50.3	73504	61918	0.842	1.765	1.487
S-T	9	hoop	35.9	30.5	0.002	0.0169	452	302	10	76	66	71595	56803	0.793	3.092	2.453
S-T	10	spiral	35.5	30.2	0.002	0.0230	452	210	10	79	69	34619	24178	0.698	4.278	2.987
S-T	11	spiral	35.5	30.2	0.002	0.0167	452	210	10	109	99	34619	20222	0.584	3.100	1.811
S-T	12	spiral	35.5	30.2	0.002	0.0223	607	212	8	41	33	35281	30003	0.850	7.017	5.967
S-T	13	spiral	35.5	30.2	0.002	0.0170	607	212	8	53	45	35281	28190	0.799	5.428	4.337
S-T	14	spiral	35.5	30.2	0.002	0.0115	607	212	8	79	71	35281	24455	0.693	3.642	2.524
S-T	15	spiral	35.5	30.2	0.002	0.0084	607	212	8	109	101	35281	20475	0.580	2.639	1.532
S-T	17	spiral	35.5	30.2	0.002	0.0114	593	214	5.7	41	35.3	35950	30264	0.842	3.448	2.902
S-T	18	spiral	35.5	30.2	0.002	0.0087	593	214	5.7	53	47.3	35950	28443	0.791	2.667	2.110
S-T	19	hoop	35.5	30.2	0.002	0.0170	607	212	5.7	53	47.3	35281	27848	0.789	2.756	2.175
S-T	20	spiral	34.9	29.7	0.002	0.0179	607	169	8	64	56	22420	15607	0.696	5.639	3.925
S-T	21	spiral	34.9	29.7	0.002	0.0115	629	171	6.4	64	57.6	22954	15873	0.692	3.696	2.556
S-T	22	spiral	34.9	29.7	0.002	0.0115	629	171	6.4	64	57.6	22954	15873	0.692	3.696	2.556
S-T	23	spiral	34.9	29.7	0.002	0.0086	629	171	6.4	86	79.6	22954	13513	0.589	2.751	1.619
S-T	24	spiral	34.9	29.7	0.002	0.0168	629	171	6.4	43	36.6	22954	18304	0.797	5.501	4.387
S-T	25	spiral	34.9	29.7	0.002	0.0168	629	171	6.4	43	36.6	22954	18304	0.797	5.501	4.387
S-T	26	spiral	34.9	29.7	0.002	0.0168	629	171	6.4	43	36.6	22954	18304	0.797	5.501	4.387
S-T	27	spiral	34.9	29.7	0.002	0.0093	605	172	4.8	43	38.2	23223	18352	0.790	2.959	2.338
S-T	28	hoop	34.9	29.7	0.002	0.0115	629	171	6.4	64	57.6	22954	15873	0.692	3.696	2.556
M-P-P	1	spiral	28	29	0.0015	0.0250	340	438	12	41	29	150598	140792	0.935	4.280	4.002
M-P-P	2	spiral	28	29	0.0015	0.0150	340	438	12	69	57	150598	131637	0.874	2.543	2.223
M-P-P	3	spiral	28	29	0.0015	0.0100	340	438	12	103	91	150598	120934	0.803	1.704	1.368
M-P-P	4	spiral	28	29	0.0015	0.0060	320	440	10	119	109	151976	116659	0.768	0.960	0.737
M-P-P	5	spiral	28	29	0.0015	0.0200	320	440	10	36	26	151976	143128	0.942	3.172	2.987
M-P-P	6	spiral	28	29	0.0015	0.0200	307	434	16	93	77	147859	122790	0.830	3.057	2.539
M-P-P	7	spiral	31	32	0.0014	0.0200	340	438	12	52	40	150598	137158	0.911	3.375	3.074
H-K-N-T	SC1	hoop		18.5	0.002	0.0039	235	200	6	150	144	31400	12861	0.410	0.443	0.181
H-K-N-T	SC2	hoop		18.5	0.002	0.0058	235	200	6	100	94	31400	18376	0.585	0.664	0.389
H-K-N-T	SC3	hoop		18.5	0.002	0.0117	235	200	6	50	44	31400	24872	0.792	1.328	1.052
H-K-N-T	SC4	hoop		18.5	0.002	0.0233	235	200	6	25	19	31400	28488	0.907	2.656	2.410
H-K-N-T	SC5	hoop		18.5	0.002	0.0466	235	200	6	12.5	6.5	31400	30388	0.968	5.313	5.142
H-K-N-T	LC1	hoop		28.8	0.002	0.0019	295	500	10	300	290	196250	98930	0.504	0.309	0.156
H-K-N-T	LC2	hoop		28.8	0.002	0.0039	295	500	10	150	140	196250	145147	0.740	0.618	0.457
H-K-N-T	LC3	hoop		28.8	0.002	0.0058	295	500	10	100	90	196250	162515	0.828	0.926	0.767
H-K-N-T	LC4	hoop		28.8	0.002	0.0116	295	500	10	50	40	196250	180864	0.922	1.853	1.707
H-K-N-T	LC5	hoop		28.8	0.002	0.0034	295	500	13	300	287	196250	99767	0.508	0.522	0.265
H-K-N-T	LC6	hoop		28.8	0.002	0.0054	295	500	16	300	284	196250	100609	0.513	0.790	0.405
A-S	II-b	spiral		26.2	0.0021		413	75	3.07	25.4	22.33	4416	3199	0.724	3.208	2.324
A-S	II-c	spiral		26.2	0.0021		413	75	3.07	12.7	9.63	4416	3867	0.876	6.416	5.619
A-S	III-b	spiral		37.9	0.0022		413	75	3.07	38.1	35.03	4416	2594	0.587	2.139	1.256
A-S	III-c	spiral		37.9	0.0022		413	75	3.07	25.4	22.33	4416	3199	0.724	3.208	2.324
A-S	III-d	spiral		37.9	0.0022		413	75	3.07	12.7	9.63	4416	3867	0.876	6.416	5.619
A-S	IV-b	spiral		51.7	0.0025		413	75	3.07	38.1	35.03	4416	2594	0.587	2.139	1.256
A-S	IV-c	spiral		51.7	0.0025		413	75	3.07	25.4	22.33	4416	3199	0.724	3.208	2.324

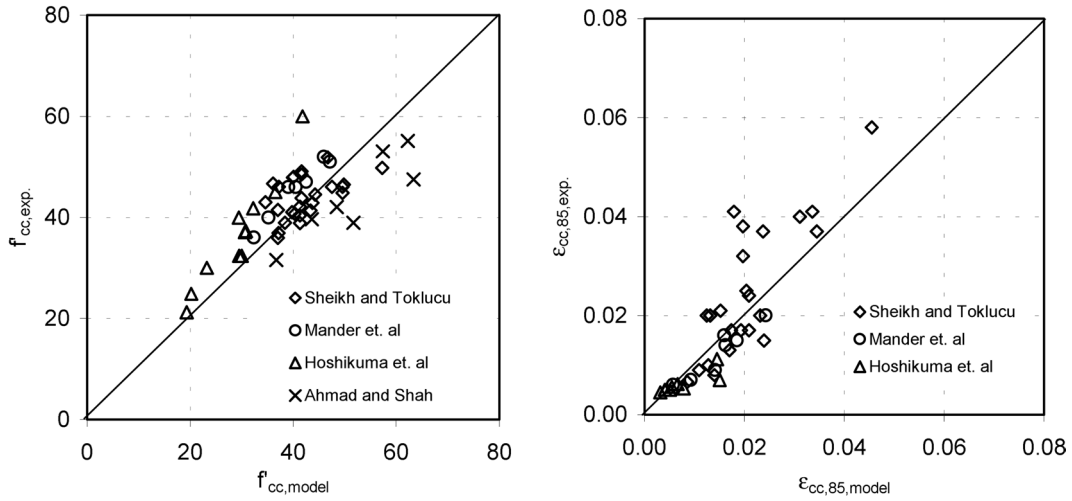


Fig. 14 Experimental and predicted values of  $f'_{cc}$  and  $\epsilon_{cc,85}$

Table 5 Comparison of predicted strength and deformation characteristics with experimental data

Researcher	Specimen	$f'_{cc,model}$	$\epsilon_{cc,85,model}$	$f'_{cc,exp}$	$\epsilon_{cc,85,exp}$	$f'_{cc,exp}/f'_{cc,model}$	$\epsilon_{cc,85,model}/\epsilon_{cc,85,exp}$
		MPa		MPa			
S-T	1	46.76	0.0278	51.85	NA	1.11	NA
S-T	2	41.64	0.0197	48.50	0.038	1.16	1.93
S-T	3	37.08	0.0125	41.48	0.020	1.12	1.61
S-T	4	34.61	0.0085	43.01	0.007	1.24	0.77
S-T	5	44.30	0.0239	44.53	0.015	1.01	0.63
S-T	6	39.95	0.0170	47.89	0.013	1.20	0.76
S-T	7	36.09	0.0109	46.67	0.009	1.29	0.83
S-T	8	37.25	0.0127	46.06	0.010	1.24	0.79
S-T	9	41.64	0.0197	49.11	0.032	1.18	1.62
S-T	10	43.76	0.0238	42.88	0.037	0.98	1.56
S-T	11	38.42	0.0152	38.96	0.021	1.01	1.38
S-T	12	57.29	0.0455	49.83	0.058	0.87	1.28
S-T	13	49.89	0.0336	46.51	0.041	0.93	1.22
S-T	14	41.66	0.0204	43.79	0.025	1.05	1.23
S-T	15	37.15	0.0132	36.91	0.020	0.99	1.52
S-T	17	43.38	0.0231	41.37	0.020	0.95	0.86
S-T	18	39.78	0.0174	41.07	0.017	1.03	0.98
S-T	19	40.08	0.0178	48.02	0.041	1.20	2.30
S-T	20	47.52	0.0311	46.04	0.040	0.97	1.29
S-T	21	41.30	0.0209	40.39	0.017	0.98	0.81
S-T	22	41.30	0.0209	38.91	NA	0.94	NA
S-T	23	37.05	0.0140	35.94	0.008	0.97	0.57
S-T	24	49.62	0.0345	46.04	0.037	0.93	1.07
S-T	25	49.62	0.0345	44.85	NA	0.90	NA
S-T	26	49.62	0.0345	46.04	NA	0.93	NA
S-T	27	40.32	0.0193	40.70	0.017	1.01	0.88
S-T	28	41.30	0.0209	42.17	0.024	1.02	1.15

Table 5 Continued

Researcher	Specimen	$f'_{cc,model}$	$\epsilon_{cc,85,model}$	$f'_{cc,exp}$	$\epsilon_{cc,85,exp}$	$f'_{cc,exp}/f'_{cc,model}$	$\epsilon_{cc,85,model}/\epsilon_{cc,85,exp}$
		MPa		MPa			
M-P-P	1	47.17	0.0243	51.00	0.020	1.08	0.82
M-P-P	2	39.09	0.0141	46.00	0.009	1.18	0.64
M-P-P	3	35.21	0.0093	40.00	0.007	1.14	0.75
M-P-P	4	32.34	0.0057	36.00	0.006	1.11	1.05
M-P-P	5	42.56	0.0185	47.00	0.015	1.10	0.81
M-P-P	6	40.53	0.0159	46.00	0.016	1.14	1.00
M-P-P	7	45.95	0.0162	52.00	0.014	1.13	0.86
H-K-N-T	SC1	19.32	0.0042	21.20	0.005	1.10	1.20
H-K-N-T	SC2	20.26	0.0066	24.90	0.006	1.23	0.94
H-K-N-T	SC3	23.28	0.0145	30.00	0.011	1.29	0.77
H-K-N-T	SC4	29.44	0.0307	40.00	NA	1.36	NA
H-K-N-T	SC5	41.84	0.0631	60.00	NA	1.43	NA
H-K-N-T	LC1	29.51	0.0032	32.40	0.005	1.10	1.41
H-K-N-T	LC2	30.87	0.0055	37.30	0.006	1.21	1.02
H-K-N-T	LC3	32.28	0.0079	41.80	0.005	1.29	0.67
H-K-N-T	LC4	36.55	0.0150	45.00	0.007	1.23	0.47
H-K-N-T	LC5	30.00	0.0040	32.40	0.005	1.08	1.24
H-K-N-T	LC6	30.64	0.0051	37.10	0.005	1.21	0.98
A-S	II-b	36.75	0.0226	31.56	NA	0.86	NA
A-S	II-c	51.71	0.0516	38.93	NA	0.75	NA
A-S	III-b	43.60	0.0102	39.62	NA	0.91	NA
A-S	III-c	48.45	0.0170	42.03	NA	0.87	NA
A-S	III-d	63.41	0.0381	47.54	NA	0.75	NA
A-S	IV-b	57.40	0.0092	53.05	NA	0.92	NA
A-S	IV-c	62.25	0.0149	55.12	NA	0.89	NA

## 8. Conclusions

The results of concentric compression tests on nearly full size confined concrete columns with circular cross-section are outlined with emphasis on the failure pattern. The experimental results are evaluated by considering the inelastic buckling and strain hardening of longitudinal reinforcing bars. Based on the experimental data, a simple trilinear stress-strain relationship is proposed for the axial stress – axial strain relationship of confined concrete. Although the proposed model may be among the simplest ones available in the literature, the axial stress – axial strain relationships predicted by the model are in good agreement with the experimental data obtained by the authors, as well as other experimental data available in the literature. However, it should be noted that the validity of the model is limited to the range of parameters considered in the experimental study carried out by the authors.

## Acknowledgements

The writers A. Ilki and P. Ozdemir, acknowledge Japan International Cooperation Agency for supporting their research in the Building Research Institute, Tsukuba, Japan.

## References

- Ahmad, S.H. and Shah, S.P. (1982), "Stress-strain curves of concrete confined by spiral reinforcement", *J. of the American Concrete Institute*, **79**(6), 484-490.
- Ahmad, S.H. and Shah, S.P. (1985), "Behavior of hoop confined concrete under high strain rates", *J. of the American Concrete Institute*, **82**, 634-647.
- Assa, B. and Nishiyama, M. (1998), "Prediction of load-displacement curve of high-strength concrete columns under simulated seismic loading", *ACI Struct. J.*, **95**(5), 547-557.
- Braga, F. and Laterza, M. (1998), "A new approach to the confinement of R/C columns", *Proc. of Eleventh European Conf. on Earthquake Engineering*, Paris, September.
- Chang, G.A. and Mander, J.B. (1994), "Seismic energy fatigue damage analysis of bridge columns: Part I – Evaluation of seismic capacity", Technical Report, NCEER-94-0006, State University of New York at Buffalo, NY.
- Cusson, D. and Paultre, P. (1995), "Stress-strain model for confined high-strength concrete", *J. Struct. Eng.*, ASCE, **121**(3), 468-477.
- Dilger, W.H., Koch, R. and Kowalczyk, R. (1984), "Ductility of plain and confined concrete under different strain rates", *J. of the American Concrete Institute*, **81**, 73-81.
- Hoshikuma, J., Kawashima, K., Nagaya, K. and Taylor, A.W. (1997), "Stress-strain model for confined reinforced concrete in bridge piers", *J. Struct. Eng.*, ASCE, **123**(5), 624-633.
- Hsu, L.S. and Hsu, C.T.T. (1994), "Complete stress-strain behaviour of high-strength concrete under compression", *Magazine of Concrete Research*, **46**(169), 301-312.
- Ilki, A., Ozdemir, P. and Fukuta, T. (1997), "Confinement effect of reinforced concrete columns with circular cross-section", BRI Research Paper, 143, Building Research Institute, Tsukuba.
- Ilki, A., Ozdemir, P. and Fukuta, T. (1998), "Observed behavior of confined concrete under compression", *Proc. of 11th European Conf. on Earthquake Engineering*, Paris, France, on CD-ROM.
- Ilki, A. (1999), "A compilation on the stress-strain relationships of confined concrete", Technical Report No. TDV/TR022/36, Turkish Earthquake Foundation, Istanbul, (in Turkish).
- Ilki, A. and Kumbasar, N. (2001), "A comparison between experimental data and analytical models for confined concrete", *Technical Journal of Turkish Chamber of Civil Engineers*, **12**(3), 2419-2433, (in Turkish).
- Kent, D.C. and Park, R. (1971), "Flexural members with confined concrete", *J. Struct. Div.*, ASCE, **97**(ST7), 1969-1990.
- Mander, J.B. (1983), "Seismic design of bridge piers", A thesis submitted in partial fulfillment of the requirements for the Degree of Doctor of Philosophy in Civil Engineering, University of Canterbury, Christchurch.
- Mander, J.B., Priestley, M.J.N. and Park, R. (1988a), "Observed stress-strain behavior of confined concrete", *J. Struct. Div.*, **114**(8), 1827-1849.
- Mander, J.B., Priestley, M.J.N. and Park, R. (1988b), "Theoretical stress-strain model for confined concrete", *J. Struct. Div.*, ASCE, **114**(8), 1804-1826.
- Mau, S.T. and El-Mabsout, M. (1989), "Inelastic buckling of reinforcing bars", *J. Eng. Mech.*, ASCE, **115**(1), 1-17.
- Mau, S.T. (1990), "Effect of tie spacing on inelastic buckling of reinforcing bars", *ACI Struct. J.*, **87**(6), 671-677.
- Monti, G. and Nuti, C. (1992), "Nonlinear cyclic behavior of reinforcing bars including buckling", *J. Struct. Eng.*, ASCE, **118**(12), 3268-3284.
- Mugurama, H., Watanabe, F., Iwashimizu, T. and Mitsueda, R. (1983), "Ductility improvement of high strength concrete by lateral confinement", *Transactions of Japan Concrete Institute*, **5**, 403-410.

- Mugurama, H., Watanabe, F. and Komuro, T. (1990), "Ductility improvement of high-strength concrete columns with lateral confinement," In *ACI Spec. Publ.*, **SP-121-4**, Am. Conc. Inst., Detroit, Mich., 47-60.
- Park, R., Priestley, M.J.N. and Gill, W.D. (1982), "Ductility of square-confined concrete columns", *J. Struct. Div.*, ASCE, **108**(ST4), 929-950.
- Priestley, M.J.N., Park, R. and Potangaroa, R.T. (1981), "Ductility of spirally confined columns", *J. Struct. Div.*, ASCE, **107**(ST1), 181-202.
- Rodriguez, M.E., Botero, J.C. and Villa, J. (1999), "Cyclic stress-strain behavior of reinforcing steel including effect of buckling", *J. Struct. Eng.*, ASCE, **125**(6), 605-612.
- Saatcioglu, M. and Razvi, S.R. (1992), "Strength and ductility of confined concrete", *Struct. J.*, ASCE, **118**(6), 1590-1607.
- Saatcioglu, M., Salamat, A.H. and Razvi, S.R. (1995), "Confined columns under eccentric loading", *J. Struct. Eng.*, ASCE, **121**(11), 1547-1556.
- Sakai, K. and Sheikh, S.A. (1989), "What do we know about confinement in reinforced concrete columns?", *ACI Struct. J.*, **86**(2), 192-207.
- Sargin, M., Ghosh, K. and Handa, V.K. (1971), "Effects of lateral reinforcement upon the strength and deformation properties of concrete," *Magazine of Concrete Research*, **23**(75-76), 99-110.
- Sheikh, S.A. (1982), "A comparative study of confinement models", *J. of the American Concrete Institute*, **79**(3), 296-305.
- Sheikh, S.A. and Uzumeri, S.M. (1982), "Analytical model for concrete confinement in tied columns", *J. Struct. Div.*, ASCE, **108**(ST12), 2703-2722.
- Sheikh, S.A. and Toklucu, M.T. (1993), "Reinforced concrete columns confined by circular spirals and hoops", *ACI Struct. J.*, **90**(5), 542-553.
- Vallenas, J., Bertero, V.V. and Popov, E.P. (1977), "Concrete confined by rectangular hoops subjected to axial loads", Report No. UBC/EERC-77/13, University of California, Berkeley.
- Yalcin, C. and Saatcioglu, M. (2000), "Inelastic analysis of reinforced concrete columns", *Comput. Struct.*, **77**, 539-555.

## Notation

$A_{cc}$	: cross-sectional area confined by transverse reinforcement
$A_e$	: cross-sectional area effectively confined by transverse reinforcement
$A_s$	: cross-sectional area of longitudinal reinforcing bars
$A_{sh}$	: cross-sectional area of transverse reinforcing bars
$D_c$	: diameter of the confined cross-section from center to center of transverse reinforcement
$f'_c$	: standard cylinder concrete compressive strength
$f'_{cc}$	: confined concrete compressive strength
$f'_{cc,model}$	: confined concrete compressive strength determined by Eq. (10)
$f'_{co}$	: unconfined concrete compressive strength of the member
$f_l$	: lateral pressure provided by transverse reinforcement
$f'_l$	: effective lateral pressure provided by transverse reinforcement
$F_s$	: compressive force of the longitudinal reinforcement
$f_{sh}$	: axial stress of the reinforcing steel at the beginning of strain hardening
$f_{su}$	: tensile strength of the longitudinal reinforcement
$f_{s/Du}$	: limiting stress in compression reinforcement
$f_y$	: yield strength of the longitudinal reinforcement
$f_{yh}$	: yield strength of the transverse reinforcement
$k_e$	: confinement effectiveness coefficient

- $s$  : spacing between transverse bars  
 $s'$  : clear spacing between transverse bars  
 $\epsilon_c$  : axial concrete strain  
 $\epsilon_{cc}$  : concrete strain corresponding to confined concrete compressive strength  
 $\epsilon_{cc,85}$  : concrete strain corresponding to the stress that is 85% of the confined concrete compressive strength  
 $\epsilon_{cc,85,model}$ : concrete strain corresponding to the stress that is 85% of the confined concrete compressive strength determined by Eq. (11) or (12)  
 $\epsilon_{co}$  : concrete strain corresponding to unconfined concrete compressive strength  
 $\epsilon_s$  : axial strain of the steel reinforcement  
 $\epsilon_{sh}$  : axial strain of the steel reinforcement at the beginning of strain hardening  
 $\epsilon_{su}$  : ultimate strain for the steel reinforcement  
 $\epsilon_{s/Du}$  : limiting strain in compression reinforcement  
 $\epsilon_y$  : yield strain for the steel reinforcement  
 $\phi_l$  : diameter of the longitudinal reinforcing bars  
 $\phi_t$  : diameter of the transverse reinforcing bars  
 $\rho_{sh}$  : the volumetric ratio of the transverse reinforcement  
 $\sigma_c$  : concrete stress  
 $\sigma_s$  : steel stress